Elsevier Editorial System(tm) for European Journal of Medicinal Chemistry
Manuscript Draft

Manuscript Number: EJMECH-D-18-02000R1

Title: Designing anticancer copper(II) complexes by optimizing 2-pyridine-thiosemicarbazone ligands

Article Type: Research Paper

Keywords: Cu(II) complexe; thiosemicarbazone; anticancer; p53; telomerase.

Corresponding Author: Professor Hong Liang, Ph.D

Corresponding Author's Institution:

First Author: Jungang Deng

Order of Authors: Jungang Deng; Ping Yu; Zhenlei Zhang; Jun Wang; Jinhua Cai; Na Wu; Hongbin Sun; Hong Liang, Ph.D; Feng Yang

Abstract: To develop potential next-generation metal anticancer agents, we designed and synthesised five Cu(II) 2-pyridine-thiosemicarbazone complexes by modifying the hydrogen atom at the N-4 position of ligands, and then investigated their structure-activity relationships and anticancer mechanisms. Modification of the N-4 position with different groups caused significant differences in cellular uptake and produced superior antitumor activity. Cu complexes arrested the cell cycle at S phase, leading to down-regulation of levels of cyclin and cyclin-dependent kinases and up-regulation of expression of cyclin-dependent kinase inhibitors. Cu complexes exerted chemotherapeutic effects via activating p53 and inducing production of reactive oxygen species to regulate expression of the B-cell lymphoma-2 family of proteins, causing a change in the mitochondrial membrane potential and release of cytochrome c to form a dimer with apoptosis protease activating factor-1, resulting in activation of caspase-9/3 to induce apoptosis. In addition, Cu complexes inhibited telomerase by down-regulating the c-myc regulator gene and expression of the human telomerase reverse transcriptase.

*Graphical Abstract (for review)

Click here to download high resolution image

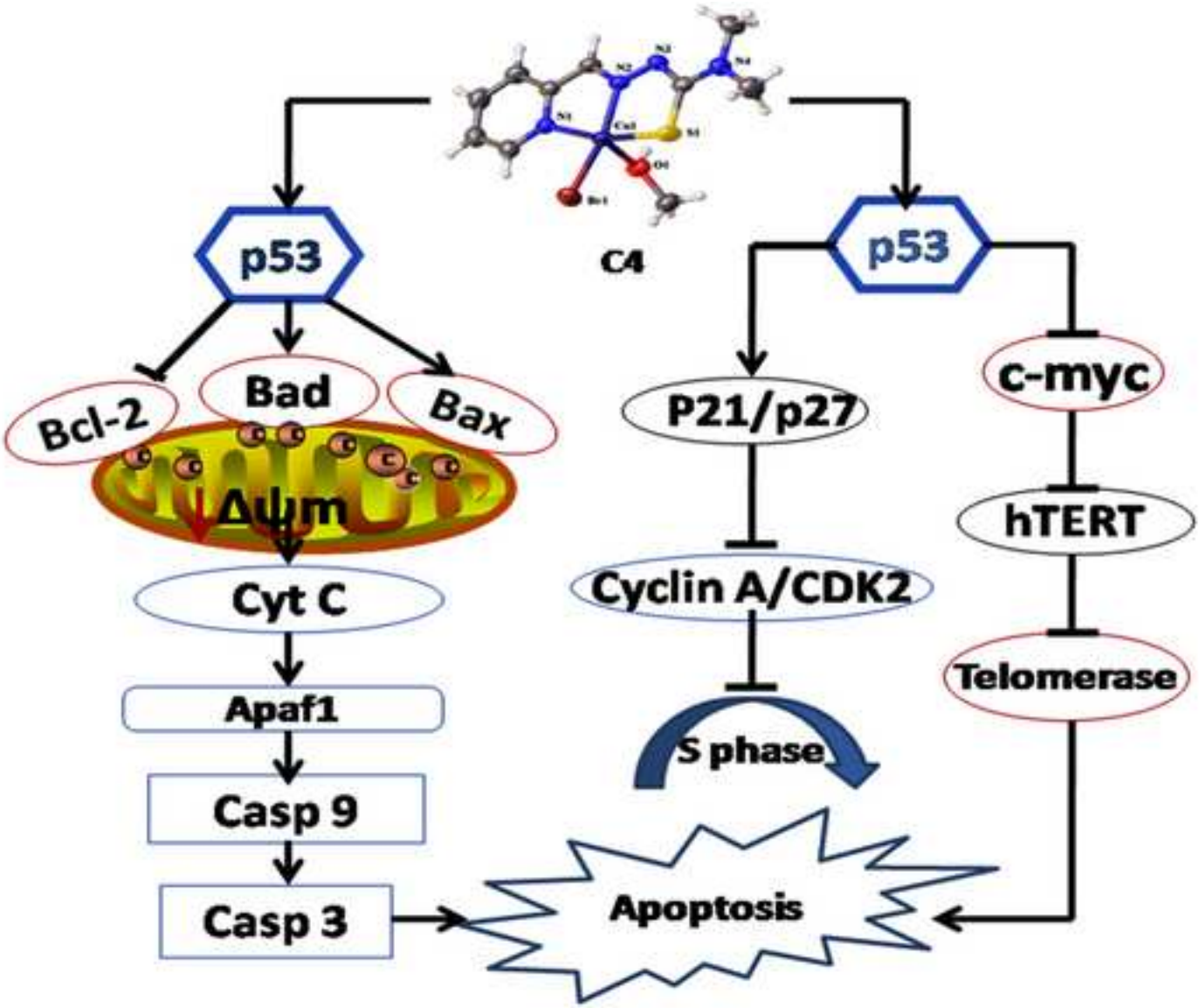

The complexes induce apoptosis of cancer cell via: 1) p53-mediatied mitochondrial pathway ; 2) inhibite telomerase by regulating c-myc regulator gene and the human telomarase reverse transcriptase (hTERT).

Highlights

- Five Cu(II) complexes modified at the N-4 position of thiosemicarbazones were synthesized.
- Cu complexes have high anticancer activity.
- Cu complexes arrest the cell at S-phase and inhibit the action of telomerase.
- Cu complexes induce the cell apoptosis *via* p53-mediated mitochondrial pathway.

Designing anticancer copper(II) complexes by optimizing 2-pyridine-thiosemicarbazone ligands

Jungang Deng[1], Ping Yu[1], Zhenlei Zhang[1], Jun Wang[1], Jinhua Cai[2], Na Wu[1], Hongbin Sun[1, 3], Hong Liang[1]*, Feng Yang[1]*

[1] State Key Laboratory for the Chemistry and Molecular Engineering of Medicinal Resources, Ministry of Science and Technology of China. Guangxi Normal University, Guilin, Guangxi, China.

[2] College of Chemistry & Chemical Engineering, Jinggangshan University, Jian, Jiangxi, China.

[3] Jiangsu Key Laboratory of Drug Discovery for Metabolic Disease, China Pharmaceutical University, Nanjing, Jiangsu, China.

*Corresponding author:

Hong Liang, hliang@mailbox.gxnu.edu.cn

Feng Yang, fyang@mailbox.gxnu.edu.cn

Phone/Fax: 86-773-584-8836

Address: 15 Yucai Road, Guilin, Guangxi, China.

Zip code: 541004

Keywords*:* Cu(II) complexe; thiosemicarbazone; anticancer; p53; telomerase.

Abstract

To develop potential next-generation metal anticancer agents, we designed and synthesised five Cu(II) 2-pyridine-thiosemicarbazone complexes by modifying the hydrogen atom at the N-4 position of ligands, and then investigated their structure-activity relationships and anticancer mechanisms. Modification of the N-4 position with different groups caused significant differences in cellular uptake and produced superior antitumor activity. Cu complexes arrested the cell cycle at S phase, leading to down-regulation of levels of cyclin and cyclin-dependent kinases and up-regulation of expression of cyclin-dependent kinase inhibitors. Cu complexes exerted chemotherapeutic effects via activating p53 and inducing production of reactive oxygen species to regulate expression of the B-cell lymphoma-2 family of proteins, causing a change in the mitochondrial membrane potential and release of cytochrome c to form a dimer with apoptosis protease activating factor-1, resulting in activation of caspase-9/3 to induce apoptosis. In addition, Cu complexes inhibited telomerase by down-regulating the *c-myc* regulator gene and expression of the human telomerase reverse transcriptase.

1 Introduction

Since *cisplatin* began being used as an anticancer drug in the 1970s, most chemotherapy drugs in clinical and preclinical studies are platinum-based complexes [1-8]. However, drug resistance and adverse side effects were common in *cisplatin* chemotherapy, therefore, scientists focused on developing novel metal complexes with better antitumor activity, fewer side effects, and reduced drug resistance to replace *cis*platin therapy [9]. In recent years, several transition-metal complexes have been developed as antitumor treatments, and the most promising of these complexes are based on copper [10, 11], ruthenium [12, 13], and gallium [14-16]. The coordination complexes of ruthenium and gallium have also entered clinical trials [17-19].

Copper, as the active centre of many enzymes, plays an important role in development and function of human organs and tissues [20-22]. To date, copper-based complexes have been extensively synthesised and investigated as anticancer agents because of their high antitumor activity and advantages relative to other metal anticancer complexes [23-38]. Thiosemicarbazones are formed by a condensation reaction of thiosemicarbazide and aldehydes or ketones. Pharmacological studies have demonstrated that thiosemicarbazones present a variety of biological activities [39, 40]. Thiosemicarbazones contain nitrogen and sulphur atoms with strong coordination ability, and can form various complexes with novel structures. Metal complexes derived from thiosemicarbazone ligands exhibit high

anticancer activity [41-44]. Currently, copper complexes derived from thiosemicarbazides have become a potential research hotspot [45-47]. Copper thiosemicarbazone complexes can produce reactive oxygen species, and act against topoisomerase II, DNA, and other potential targets in the nucleus [48]. Hence, the copper thiosemicarbazone complex is a promising candidate for developing ideal non-platinum and multi-target antitumor drugs.

Considering above factors, we synthesised five Cu(II) complexes with ligand/Cu at a ratio of 1:1 via modification at the N-4 position (Scheme 1), and characterised their structures using X-ray crystallography, elemental analysis, infrared spectroscopic analysis, and electrospray ionization-mass spectrometry. Subsequently, we investigated their associated structure-activity relationship. The five complexes identified demonstrated marked toxicity. Finally, we confirmed their multi-target anticancer mechanisms. The selected complex C4 caused apoptosis via the p53-mediated mitochondrial pathway and telomerase inhibition by regulating the expression of *c-myc* regulator gene and hTERT.

2 Results

2.1 Design and structure of five Cu complexes

Previous research showed that aldehyde-thiosemicarbazones were more advantageous than ketone-thiosemicarbazones, the latter being less active and toxic [39]. These compounds present a variety of biological activities, and these activities can increase after the N-4 position is modified to obtain

different derivatives, such as those containing hexatomic or heptatomic rings, or monocyclic or bicyclic derivatives. Based on these findings, we selected 2-pyridine-thiosemicarbazone to design and synthesise five novel Cu(II) complexes by modification of the N-4 position.

The complexes C1-C5 were prepared via the copper salt reaction with L1-L5, respectively, in methanol, stirred, and refluxed at 65 °C for 6 h. The solvent evaporation method was used to prepared crystals. Furthermore, the structures of the Cu(II) complexes were identified by X-ray crystallography as shown in Table 1. The crystal structure identified showed that the copper centres of the C1, C2, and C3 complexes were tetra-coordinated by two nitrogen atoms, one sulphur atom of chelating Schiff base ligand, and one halogen atom or one nitrate ion. Moreover, the copper centres of C4 and C5 were penta-coordinated by two nitrogen atoms, one sulphur atom of chelating thiosemicarbazone, one halogen atom or one nitrate ion, and one methanol molecule (Figure 1). The five complexes crystallise with different space groups, *P*-1, *C*2/*c*, $P2_1/c$, *P*-1, and *P*-1, respectively. The selected bond lengths are shown in Table S1.We found no obvious vibration for the Cu1-N1 bond (2.017Å-2.048Å), Cu1-N2 bond (1.959Å-1.994Å), and Cu1-S1 bond (2.2366Å-2.2744Å).The angle of N-Cu-N was in the range of 80.39-81.19˚(C1-C5). The angle of N(1)-Cu-S was in the range of 161.46-164.10˚ (C1-C5). The angle of N(2)-Cu-S was in the range of 83.33-83.68˚, and there were no major changes in the bond angles for each complex.

2.2 Stability of Cu complexes

UV-Vis spectroscopy was employed to study the stability of complexes [49]. Briefly, the complexes were dissolved in the PBS for 0, 24, and 48 h, and detected by UV-Vis spectroscopy. The results demonstrated that the UV-Vis spectra of the five complexes show no significant changes in spectral characteristics and peak absorption over time (Figure S1), which suggested that the five complexes are stable in PBS for 48 hours at room temperature.

2.3 Structure-activity relationships of Cu complexes in vitro

Six cell lines including a normal liver cell line (MGC80-3, HepG2, SK-OV-3, NCI-H460 and HL-7702) were employed to study the antitumor activity of the 2-pyridine-thiosemicarbazone ligands and their complexes *in vitro*.IC_{50} values were determined using the colourimetric assay, MTT (3-(4,5-dimethylthiazol-2-yl)-2,5-diphenyltetrazolium bromide) tetrazolium). As shown in Table 2, Cu(II) complexes are more cytotoxic to cancer cells relative to the corresponding ligand because of chelation of ligand to Cu^{2+}. All Cu(II) complexes exhibited considerable antitumor activity with IC_{50} values from 0.84 to 12.11 μM. Compared with C1, the activity of the complexes increased by 9-, 11- and 10- fold via introduction of a benzene ring (C2),formation of a piperidine ring with N-4 (C3), or apyrrolidine ring (C5) at the N-4 position in MGC80-3 cells. Introduction of two methyl groups at N-4 carrying a lead group increased the activity by more than 14-fold, which showed that the modified complexes have better activity against selected tumour cells.

Inductively coupled plasma (ICP-MS) results demonstrated that the total

intracellular copper contents were 11.94-20.81nmol (Figure 2). Relative to C1, the total concentration of the N4-modified complexes that were absorbed into cells increased to 51.21%, 40.59%, 74.28%, and 41.89%, respectively. However, there were no significant differences in the concentration of each complex distributed to the mitochondria (3.24-3.73 nmol), whereas the concentration in the nucleus increased to 31.85%, 28.38%, and 27.91% after the cells were treated with C3, C4, andC5, respectively, for 24 h. Similarly, the concentration of C2-C5 in the cytoplasm increased significantly resulting from modification at the N-4 position (Figure 2). These results showed that modifications at the N-4 position affect the amount of complex absorbed into cells and can lead to differences in antitumor activity.

2.4 Confirmation of anticancer mechanisms of Cu complexes

Apoptosis is a complex process with multiple pathways regulated by multiple proteins. The p53 protein, a nuclear transcription factor, plays an important role in regulating a wide variety of genes [50-52].A downstream response factor of p53, p21 expression is significantly increased following p53 activation, leading to cell cycle arrest. In the mitochondria-induced apoptosis pathway, p53 can activate the apoptosis regulator, Bcl-2-like protein 4, Bax, to form a heterodimer with Bcl-2 as an apoptotic activator [53, 54]. Bax increases the anion channel open probability, and induces loss of mitochondrial membrane potential ($\Delta\psi_m$), ultimately promotes release of cytochrome c (Cyt c). In addition, p53 can activate the Bcl-2-associated death promoter. Bad, by linking the protein with dephosphorylated-Badto

form a complex, and promote release of Cyt c [55, 56]. In the nucleus, p53 can bind the promoter of c-myc and promote histonedeacetylation, thereby inducing the repression of c-myc [57].

2.4.1 P53-regulates the levels of cell cycle regulators and promotes the cell cycle

Cell cycle was examined by flow cytometry. Cell cycle analysis clearly shows that the C1 complex blocks the cell cycle in the G1 phase (Figure 3A). The cell population in the G1 phase increased to 11% and 12% after treatment with 6 μM and 12 μM of the C1 complex, respectively. The C4 complex arrested the cells in the G1/S phase when used at a concentration of 0.4 μM and in the S phase with a concentration of 0.8 μM. In comparison with control cells, the G1/S populations increased 8.55% and 1.36% after the cells were treated with C4 at 0.4μM, and S populations increased 14.07% after the cells were treated with C4 at 0.8 μM.

The cell cycle is regulated by cyclin and cyclin-dependent kinases (CDKs); cyclin A, cdc25 A, and CDK2, which are closely associated with S phase. Cdc25 A activates CDK2 by dephosphorylation and promotes cell cycle progression [58, 59]. Western blot analysis using anti-cdc25A, cyclin A, and CDK2 antibodies was used to determine whether the selected complexes affect expression of related proteins in MGC80-3 cells. As shown in Figures 3B and C, expression of these three proteins decreased at varying degrees. Therefore, we further examined expression of p21 and p27 protein levels, which act as cyclin-dependent kinase inhibitors. As showed in Figures 3B and C, expression levels of p21 and p27 increased significantly

after treatment with the C4 complex for 24 h. In particular, p21 demonstrated a 6-fold increase compared to the control group.

2.4.2 P53-regulates the levels of c-myc, hTERT, and telomerase inhibition

Telomerase is over-expressed in most tumour cells, while little to no expression is found in normal cells [60, 61]. C-myc is a member of the myc family of proteins, which are strong proto-oncogenes and regulate a range of genes including those mediating cell proliferation and apoptosis. C-myc is also the first transcription factor found to regulate the expression of hTERT, an enzyme considered to act as a rate limiting factor for telomerase activation. As such, inhibition of telomerase activity by regulating c-myc and hTERT gene expression is considered a new direction in antitumor research [62-65]. Western blot results showed that levels of c-myc were reduced by 88.08% with 12 µM C1 complex relative treatment relative to control levels (Figures 4A and B). However, there were no changes when the cells were treated with 6 µM of the C1 complex. In contrast, c-myc levels were significantly reduced by 77.63% and 80.57%when cells were treated with the C4 complex at 0.4 and 0.8 µM, respectively. In addition, expression levels of hTERT significantly decreased by 72.95% and 78.27% after the cells were treated with the C4 complex at 0.4 and 0.8 µM, respectively. In contrast, this reduction was not particularly obvious after treatment with the C1 complex (6 or 12 µM). Measurement of telomerase inhibition using the polymerase chain reaction (PCR)-based telomeric repeat amplification protocol (TRAP) assay revealed that the complexes C1 and C4 inhibited telomerase activity at rates of 17.17% and 33.73%, respectively

(Figure 4C).

2.4.3 P53-mediates anticancer mechanisms via mitochondrial pathways

Proteins belonging to the Bcl-2 family play a key role in mediating the mitochondrial apoptosis pathway by controlling mitochondrial membrane permeability [66, 67]. The p53 protein can up-regulate the pro-apoptotic proteins Bad and Bax, and down-regulate expression of Bcl-2, resulting in the dissipation of $\Delta\psi_m$ and release of Cyt c [68, 69], which is a key step in apoptosis. Moreover, Cyt c forms a dimer with apoptosis-related factor 1 (Apaf-1) and activates caspase-3/9. Flow cytometry results showed that cells treated with C1 and C4 complexes can lead to collapse of the $\Delta\psi_m$. Compared with the 3.24% $\Delta\psi_m$ of control cells, the $\Delta\psi_m$ decreased to 18.60% and 54.90% after treatment with the C1 complex at 6 μM and 12 μM, respectively. Similarly, the $\Delta\psi_m$ decreased to 12.30% and 52.90% after treatment with the C4 complex at0.4μM and 0.8 μM, respectively (Figure S3). Importantly, the decrease in $\Delta\psi_m$ was positively correlated with the dose of complex administered. Western blot results showed that levels of Apaf-1, Bad, Bax, and Cyt c increased significantly after MGC80-3 cells were treated with complex C4, while Bcl-2 levels decreased (Figures 5A and B). Meanwhile, we used the fluorescent 2,7-dichlorofluorescein (DCF) probe to evaluate the ability of the selected complexes to catalyse production of intracellular ROS in MGC80-3 cells, which can promote expression of apoptotic proteins as second messengers and induce opening of the mitochondrial permeability transition pore [70-73]. After cells were exposed to the C1 complex (6 or 12 μM) and the C4 complex (0.4 or 0.8 μM) for 24

h, cells produced a green fluorescence characteristic of activation (Figure S3).

Downstream of the mitochondrial apoptotic pathway, caspase 3 acts as an apoptotic signalling molecule as caspase 9 activation leads to caspase 3 activation [74, 75]. In this experiment, flow cytometry was used to examine activation of caspase-9/3. As shown in Figure S4, activated caspase-9 levels increased 24.93% and 31.19% after treatment with the C1 (12 μM) and C4 (0.8 μM) complexes. Similarly, activated caspase-3 levels increased 5.96% and 10.56%, respectively.

Our results showed that cells treated with two doses of the selected complexes underwent dose-dependent late apoptosis, with the percentages of the apoptotic MGC80-3 cells increasing with dose by 5.04% and 18.85% when treated with the C1 complex at6 μM and 12 μM, respectively, and by 2.65% and 29.84% when treated with the C4 complex (0.4 or 0.8 μM) as compared to the control group (Figure 5C).

2.4.4 The action of DNA cleavage studies

Many studies have shown that Schiff base copper complexes can target DNA [76, 77]. Therefore, we investigated the effects of C1 and C4 on Pbr322 plasmid DNA by gel electrophoretic separations. The results showed that a relatively high concentration of C1 did not significantly cleave DNA. In contrast, C4 relaxed Form I (supercoiled form) of DNA into Form II at 250 μM (Figure S5), implying that C4 may act against DNA in cancer cells.

3 Discussion

A common approach in drug discovery is to find a promising lead drug and modify the structure of the compound to improve performance. Structural modification can change absorption, extend duration of effect, reduce toxicity, and increase solubility, among other potential benefits.

Discovery of novel high-efficiency and low-toxicity antitumor agents from thiosemicarbazone derivatives and their complexes is a field receiving increasing amounts of attention. Studies have shown that modification at the N-4 position of thiosemicarbazides with moieties such as introducing carboxyl groups, phenyl group, forming a 5- or 6-membered aromatic heterocycle, etc. can improve anti-tumour potential of these molecules. Our experiments evaluating cellular uptake showed that complexes modified at the N-4 position were more readily absorbed into cells and distributed to the nucleus than the original complex, which may indicate the mechanisms underlying the increase in activity of the N-4 modified complexes in our studies.

Based on the complexity of tumour development, there are crossovers and compensations between signalling pathways for most tumours to maintain their growth and survival. In clinical studies, the effects of targeted therapy against a single pathway are often unsatisfactory, with activation of alternative pathways as one of the mechanisms for this effect. Multi-target drug development can achieve synergistic effects and overcome drug resistance by inhibiting multiple signalling pathways or multiple molecules upstream and/or downstream of one pathway, providing therapeutic action against multiple targets in cancer cells simultaneously. Our results showed

that the Cu N-4 modified 2-pyridine-thiosemicarbazone complexes could significantly up-regulate p21 and arrest MGC80-3 cells at S phase, and induce apoptosis by regulating $\Delta\psi_m$ via down-regulation of p53 to regulate expression of Bcl-2 family proteins. In addition, since telomerase is considered a promising target for novel anticancer drugs, C4 was shown to inhibit telomerase activity by significantly inhibiting the expression of c-myc and hTERT. Therefore, the thiosemicarbazone-based Cu complexes show promise as an avenue for development of multi-target anticancer metal pro-drugs.

4 Conclusion

To develop the next-generation metal-based anticancer agents, we designed and optimised Cu(II) tridentate 2-pyridine-thiosemicarbazone complexes by modifying the N-4 position in thiosemicarbazones. The Cu complexes not only confer marked anticancer activity, but can also directly induce cancer cell apoptosis through multiple mechanisms, including regulation of proteins related to the cell apoptosis pathway, and inhibition of telomerase activity. Our results suggested that the Cu(II) tridentate 2-pyridine-thiosemicarbazone complexes have potential as promising multi-target anticancer metal lead drugs.

5 Materials and Methods

All chemicals were provided by Energy Chemical Company (Shanghai, China).All cell lines (MGC80-3, SK-OV-3, NCI-H460, HepG2 and HL-7702) were provided by the Shanghai Institute for Biological Science (Shanghai, China). The mitochondrial membrane potential assay kit with

JC-1, the reactive oxygen species assay kit, the mitochondria isolation kit, and nuclei isolation kit were purchased from Beyotime (Jiangsu, China). Fluorescein active caspase-3 and -9 staining kits were purchased from BioVision (Milpitas, CA). The telomerase activity assay kit was provided by Genmed (Minneapolis, MN). The antibodies used in western blot were provided by Abcam (Cambridge, UK).

5.1 Synthesis of ligands

The L1-L5 ligands were prepared using previously published methods [78]. In brief, 2-pyridinecarboxaldehyde (10 mmol) MeOH solution was added to the corresponding equimolar thiosemicarbazides (10 mmol) and stirred for 6 h at 60℃, and the ligands were precipitated and filtered to obtain the L1−L5 ligands. The ligands were purified by re-crystallization. All ligands were characterised by elemental analysis, infrared spectral analysis, ^{1}H-NMR and electrospray ionization-mass spectrometry (ESI-MS; Supporting Information, Figures S6−S15).

N-methyl-2-(pyridin-2-ylmethylene)hydrazinecarbothioamide(L1): yield (1.52 g, 78%). Anal. Calcd (%) for $C_8H_{10}N_4S$: C, 49.46; H, 5.19; N, 28.84; S, 16.51. Found: C, 49.23; H, 5.02.; N, 28.68, S, 16.43. IR (KBr, cm^{-1}): 3450, 3288, 3138, 2943, 1528, 1433, 1319, 1267, 1247, 1151, 1109, 1088, 1038, 997, 928, 885, 779, 675, 623, 608, 520, 414. ^{1}H NMR (400 MHz, DMSO) δ 11.70 (s, 1H), 8.66 (d, J= 4.4 Hz, 1H), 8.56 (d, J = 4.7 Hz, 1H), 8.26 (d, J =

8.0 Hz, 1H), 8.08 (s, 1H), 7.87–7.82 (m, 1H), 7.40–7.34 (m, 1H), 3.32 (s, 3H).ESI-MS: m/z =177.0[$C_8H_{10}N_4S$-2H-CH_3]$^-$.

N-phenyl-2-(pyridin-2-ylmethylene)hydrazinecarbothioamide(L2): yield (1.81 g, 70%). Anal. Calcd (%) for $C_{13}H_{12}N_4S$:C, 60.91; H, 4.72; N, 21.86; S, 12.51. Found: C, 60.77; H, 4.61; N, 21.73; S, 12.58.IR (KBr, cm^{-1}):3307, 3124, 2952, 1597, 1551, 1524, 1468, 1326, 1287, 1256, 1189, 1160, 1109, 1077, 997, 942, 923, 754, 692, 622, 506, 480. ^{1}H NMR (400 MHz, DMSO) δ 12.03 (s, 1H), 10.25 (s, 1H), 8.59 (ddd, *J* = 4.9, 1.6, 0.9 Hz, 1H), 8.45 (d, *J* = 8.0 Hz, 1H), 8.20 (s, 1H), 7.85 (td, *J* = 7.7, 1.4 Hz, 1H), 7.59–7.53 (m, 2H), 7.42–7.34 (m, 3H), 7.24 (dd, *J* = 10.5, 4.2 Hz, 1H).ESI-MS: m/z= 179.00**[**$C_{13}H_{12}N_4S-C_6H_5]^+$.

N'-(pyridin-2-ylmethylene)piperidine-1-carbothiohydrazide(L3): yield (1.86 g, 75%). Anal. Calcd (%) for $C_{12}H_{16}N_4S$: C, 58.04; H, 6.49; N, 22.56; S, 12.91. Found: C, 58.04; H, 6.49; N, 22.56; S, 12.91. IR (KBr, cm^{-1}): 3431, 3141, 2929, 1497, 1349, 1281, 1010, 997, 894, 774, 619, 536, 515, 446, 411.^{1}H NMR (400 MHz, DMSO) δ 11.25 (s, 1H), 8.58 (dt, *J* =4.8, 1.2 Hz, 1H), 8.17 (s, 1H), 7.87–7.83 (m, 2H), 7.37 (d, *J* =4.1 Hz, 1H), 3.88 (s, 4H), 1.66–1.60 (m, 6H).ESI-MS: m/z = 249.12 [$C_{12}H_{16}N_4S$+H]$^+$.

N,N-dimethyl-2-(pyridin-2-ylmethylene)hydrazinecarbothioamide(L4): yield (1.73 g, 83%). Anal. Calcd (%) for $C_9H_{12}N_4S$: C, 51.90; H, 5.81; N, 26.90; S, 15.39. Found: C, 51.76; H, 5.88; N, 26.81; S, 15.31. IR (KBr, cm^{-1}):

3431, 3125, 2972, 1553, 1410, 1238, 1154, 1103, 1078, 1056, 900, 875, 778, 737, 620, 583, 513. ^{1}H NMR (400 MHz, DMSO) δ 11.71 (s, 1H), 8.67 (d, J = 4.3 Hz, 1H), 8.57 (d, J = 4.6 Hz, 1H), 8.26 (d, J = 8.0 Hz, 1H), 8.09 (s, 1H), 7.85 (td, J = 7.8, 1.3 Hz, 1H), 3.04 (d, J = 4.5 Hz, 6H).ESI-MS: m/z = 207.07[$C_9H_{12}N_4S-H]^-$.

N'-(pyridin-2-ylmethylene)pyrrolidine-1-carbothiohydrazide(L5):yield (1.77 g, 75%). Anal. Calcd (%) for $C_{11}H_{14}N_4S$: C, 56.38; H, 6.02; N, 23.91; S, 13.68. Found: C, 56.22; H, 6.11; N, 23.83; S, 13.62.IR (KBr, cm^{-1}): 3435, 3018, 2927, 2856, 2768, 1604, 1567, 1498, 1435, 1360, 1308, 1274, 1249, 1222, 1192, 1164, 1134, 1014, 951, 918, 885, 781, 714, 624, 518, 419.^{1}HNMR (400 MHz, DMSO) δ 11.24 (s, 1H), 8.60–8.54 (m, 1H), 8.20 (s, 1H), 7.90–7.81 (m, 2H), 7.36 (ddd, J = 6.7, 4.9, 1.4 Hz, 1H), 3.76 (s, 4H), 1.90 (s, 4H).ESI-MS: m/z = 233.09 [$C_{11}H_{14}N_4S-H]^-$.

5.2 Synthesis and characterization of Cu(II) complexes

The ligands (0.1 mmol) and the copper salts solution (0.1 mmol) were added into 20ml MeOH solution and refluxed for 6 h at 65 °C. The reaction solution was placed at room temperature to obtain crystals, and the complexes were purified by re-crystallization. The new complexes were [Cu(P4mT)Cl] (C1), [Cu(P4pT)NO_3] (C2), [Cu(P3piT)Br] (C3), [Cu(P44mT)(CH_3OH)Br] (C4), and [Cu(P3pyT)(CH_3OH)Cl] (C5). Elemental analysis, infrared spectral analysis, and ESI-MS were employed to verify the structures of the complexes (Supporting Information, Figures

S6−10, S21−25).

[Cu(P4mT)Cl] (C1): yield (23.96 mg, 82%). Anal. Calc. for $C_8H_9ClCuN_4S$: C, 32.88; H, 3.10; N, 19.17; S, 10.97. Found: C, 32.71; H, 3.01; N, 19.29; S, 10.81. IR (KBr, cm^{-1}): 3451, 1637, 1595, 1537, 1469, 1357, 1306, 1283, 1226, 1121, 1043, 608, 520. MS m/z: 334.0 $[M+H+C_2H_3N]^-$.

[Cu(P4pT)NO_3] (C2): yield (27.04 mg, 71%). Anal. Calc. for $C_{13}H_{11}CuN_5O_3S$: C, 41.00; H, 2.91 N, 18.39; S, 8.42. Found: C, 41.13; H, 2.82 N, 18.25; S, 8.31. IR (KBr, cm^{-1}): 3328, 1600, 1544, 1455, 1433, 1383, 1284, 1128, 747. MS m/z: 318.00 $[M-NO_3]^+$.

[Cu(P3piT)Br] (C3): yield (28.92 mg, 74%). Anal. Calc. for $C_{12}H_{15}BrCuN_4OS$: C, 36.88; H, 3.87; N, 14.34. Found: C, 36.76; H, 3.95; N, 14.26. IR (KBr, cm^{-1}) 3435, 1629, 1584, 1563, 1463, 1432, 1285, 1219, 11084, 1041, 991, 953, 863, 777, 618, 500, 405. MS m/z: 390.04$[M-H]^-$.

[Cu(P44mT)(CH_3OH)Br] (C4): yield (29.09 mg, 76%). Anal. Calc. for $C_{10}H_{15}BrCuN_4OS$: C, 31.46; H, 3.70; N, 14.68; S, 8.40. Found: C, 31.34; H, 3.83; N, 14.58; S, 8.31. IR (KBr, cm^{-1}) 3433, 2897, 1581, 1519, 1466, 1415, 1280, 1149, 906, 782, 644, 613. MS m/z : 350.01 for $[M-H-CH_3OH]^-$.

[Cu(P3pyT)(CH_3OH)Cl] (C5): yield (28.78 mg, 79%). Anal. Calc. for $C_{12}H_{17}ClCuN_4OS$: C, 39.67; H, 4.44; N, 15.42; S, 8.82. Found: C, 39.54; H, 4.32; N, 15.56; S, 8.73. IR (KBr, cm^{-1}): 3434, 1631, 1381, 1160, 773. MS m/z: 331.94$[M-H-CH_3OH]^-$.

5.3X-ray crystallography

A diffractometer was used to collect X-ray diffraction data for the five copper complexes. Olex2 software was employed to resolve the structure of

the complexes [79].The atoms excluding hydrogen atom are refined anisotropically. The hydrogen atom is theoretically added at the appropriate position by Olex2.The crystal data of all copper complexes are listed in Table 1. Selected bond lengths (Å) and angles (degrees) are given in Tables S1-S2.

5.4 In vitro cytotoxicity assay

Stock solutions (10 mM) of the ligands and copper complexes were prepared by dissolving the complexes in DMSO, and diluted to various concentrations with PBS. The MTT assay was employed to investigate cell toxicity [80]. Briefly, all cells were seeded in 96-well plates. After incubation for 24 h, the complexes were added to the culture medium at various concentrations and the cells were incubated for 48 h. MTT solution (10μL) was added to each well and incubated for 4 h. One-hundred microliters of DMSO was added to each well after the culture medium was removed. The absorbance was measured by an enzyme-labelling instrument and IC_{50} values were calculated.

5.5 Cellular uptake

To investigate the underlying mechanisms of the enhanced activity of the modified complexes, ICP-MS was performed to detect distribution of the complexes in cancer cells [81]. Briefly, the selected cells were treated with the five complexes at the same dose (0.8 μM) for 24 h, the mitochondria isolation kit and nuclei isolation kit were used to separate and extract the mitochondrial membrane fraction, nuclear fraction, and cytoplasm. Meanwhile, copper content in the control cells was also measured.

5.6 TRAP assay

To investigate inhibition of telomerase activity by the selected complexes, a TRAP-Silver stain assay was performed [82]. Briefly, 1×10^6 MGC80-3 cells were treated with C1 (12 μM) and C4 (0.8 μM) for 24 h. The cells were collected and telomerase was extracted according to the kit instructions. Five microliters of telomerase reaction mixture added to a final volume of 50 μL for PCR amplification. The sample was incubated at 30 °C for 30 minutes, followed by 30 cycles of 92 °C for 30 seconds, 52 °C for 30 seconds, and 72 °C for 30 seconds. Non-denaturing acrylamide gel electrophoresis (12%; 19:1) was used to isolate proteins at 180 V for 40 minutes and 220 V for 80 minutes. Gels were stained with 0.2 % $AgNO_3$andbands developed with sodium bicarbonate.

5.7 Cell cycle analysis

To study the effects of the complexes on the cell cycle of tumours, we used flow cytometry to detect changes in cell cycle distribution before and after drug treatment. Briefly, MGC80-3 cell suspension (1×10^5 cells/mL) was plated in 10-mm culture dishes and incubated for 12 h, then treated with C1 (6 or 12 μM) and C4 (0.4 or 0.8 μM) for 48 h. The cells were harvested and washed with cool PBS solution. Cells were fixed in ice-cold 70% ethanol solution and stored at -25 °C for 24 h. The cells were centrifuged and incubated with RNase A for 30 min. The cell cycle distribution was detected with a flow cytometer.

5.8 Intracellular measurements of ROS

Intracellular ROS generation was investigated using the fluorescent

probe dichloro-dihydro-fluorescein diacetate (H_2DCFH-DA) and visualised by fluorescence microscopy. The cells seeded in 6-well plates were exposed to C1 (6 or 12 μM) and C4 (0.4 or 0.8 μM) for 24 h. Cool PBS solution was used to wash the cells twice, and the cells were incubated in serum-free medium containing H_2DCFDA (2 mM), and finally washed twice using serum-free medium. A fluorescence microscope was used to observe the cell fluorescence.

5.9 Measurement of the $\Delta\psi_m$

A flow cytometer employing JC-1 probe was used to detect changes in $\Delta\psi_m$ in MGC80-3 cells. The cells in 6-well plates were exposed to C1 (6 or 12 μM) and C4 (0.4 or 0.8 μM) for 24 h, harvested, and washed twice with cool PBS solution. JC-1 stock solution was added to the cells and incubated for 30 minutes. A flow cytometer was used to detect the fluorescence of separated cells.

5.10 DNA cleavage studies

Briefly, supercoiled plasmid pBR322 DNA, Tris-HCl buffer and different concentrations of C1 and C4 (25, 100, and 250 μM) were mixed and incubated in a tube at 37 °C for 3 h. Subsequently, the loading buffer was added into the mixture. The mixture was loaded onto 1% agarose gel containing 1% (v/v) goldView II, and analysed by gel electrophoresis in 1X TBE buffer at 80 V.

5.11 Western blot analysis

The selected cells were seeded in the plate and exposed toC1 (6 or 12

μM) and C4 (0.4 or 0.8 μM) for 24 h. A lysis buffer was employed to lysethe harvested cells. 12% SDS–polyacrylamide gel electrophoresis was employed to separate proteins. Proteins were transferred to polyvinylidene difluoride (PVDF) membranes, and the membranes were incubated with different antibodies. A western blot detection system was used. Gray scale analysis was used for quantitative analysis of bands.

5.12 Determination of caspase-3/9 activity

Activation of caspase-3/9 was measured by flow cytometry employing a Fluoresce in Active Caspase-3/9 Staining Kit. Appropriate cells in six well plates were exposed for 24 h to C1and C4 at 12 μM and 0.8μM, respectively. Cells were harvested and washed with cool PBS solution, plus wash buffer containing FITC-DEVD-FMK, and incubated for 30 minutes. A flow cytometer was employed to detect caspase-3/9 activity.

5.13 Cell apoptosis assay

Annexin V/PI double staining was employed to investigate cell apoptosis, which was analysed by flow cytometry. Briefly, after treatment with C1 (6 or 12 μM) and C4 (0.4 or 0.8 μM) for 24 h, the cells were harvested and re-suspended. Annexin V-FITC and PI were added and the cells were incubated for 15 minutes and analysed by flow cytometry. The data were then analysed using FlowJo software.

5.14 Statistical analysis

Student's t-test was employed to evaluate significant differences. The data are showed as mean ± standard deviation (SD). A p-value < 0.05 was considered significant.

Acknowledgements

This work received financial support from the Natural Science Foundation of China (31460232, 21431001, 21561017, 21462004), the Natural Science Foundation of Guangxi (2017GXNSFEA198002, AD17129007), IRT_16R15, Guangxi "Bagui" scholar program to HB Sun, and High-Level Innovation Team and Distinguished Scholar program of Guangxi universities to F Yang.

References

[1] S.J. Berners-Price, Activating platinum anticancer complexes with visible light, Angew. Chem. Int. Ed. Engl. 50 (2011) 804-805.

[2] S. J. Berners-Price, L. Ronconi, P.J. Sadler, Insights into the mechanism of action of platinum anticancer drugs from multinuclear NMR spectroscopy, Prog. Nucl. Magn. Reson. Spectrosc. 49 (2006）65-98.

[3] J.R. Eckardt, D.L. Bentsion, O.N. Lipatov, I.S. Polyakov, F.R. MacKintosh, D.A. Karlin, G.S. Baker, H.B. Breitz, Phase II study of picoplatin as second-line therapy for patients with small-cell lung cancer, J. Clin. Oncol. 27 (2009) 2046-2051.

[4] S.G. Bagrova, Results of phase II clinical trial of cycloplatam in refractory solid tumors, Vopr. Onkol. 47 (2001) 752-756.

[5] M. Campone, J.M. Rademaker-Lakhai, J Bennouna, B.H. Stephen, P.N. David, H.B. Jos, J.H.M. San, Phase I and pharmacokinetic trial of AP5346, a DACH-platinum-polymer conjugate, administered weekly for three out of every 4 weeks to advanced solid tumor patients, Cancer Chemoth. Pharm. 60 (2007) 523-533.

[6]C. Ceresa, A. Bravin, G. Cavaletti, M.Pellei, C. Santini, The combined therapeutical effect of metal-based drugs and radiation therapy: the present status of research, Curr. Med. Chem. 21 (2014) 2237-2265.

[7] M.I. Koukourakis, A. Giatromanolaki, M. Pitiakoudis, G. Kouklakis, P. Tsoutsou,I. Abatrzoglou, M. Panteliadou, K. Sismanidou, E. Sivridis, T. Boulikas, Concurrent liposomal cisplatin (Lipoplatin), 5-fluorouracil and radiotherapy for the treatment of locally advanced gastric cancer: a phase I/II study, Int. J. Radiat. Oncol. 78 (2010) 150-155.

[8] N.J. Wheate, S. Walker, G.E. Craig, O. Rabbab, The status of platinum anticancer drugs in the clinic and in clinical trials, Dalton T. 39 (2010) 8113-8127.

[9] C. Sheridan, G. Brumatti, M. Elgendy, M. Brunet, S.J. Martin, An ERK-dependent pathway to Noxa expression regulates apoptosis by platinum-based chemotherapeutic drugs, oncogene 29 (2010) 6428-6411.

[10] C. Marzano, V. Gandin, M. Pellei, D. Colavito, G. Papini, G.G. Lobbia, E. DelGiudice, M. Porchia, F. Tisato, C. Santini, In vitro antitumor activity of the water soluble copper (I) complexes bearing the tris (hydroxymethyl) phosphine ligand, J. Med. Chem. 51 (2008) 798-808.

[11] M.V. Nikolic, M.Z. Mijajlovic, V.V. Jevtic, Z.R. Ratkovic, S.B. Novakovic, G.A. Bogdanovic, J. Milovanovic, A. Arsenijevic, B. Stojanovic, S.R. Trifunovic, G.P. Radic, Cytotoxicity of copper (II)-complexes with some S-Alkyl derivatives of thiosalicylic acid, Crystal structure of the binuclear copper (II)-complex with S-ethyl derivative of thiosalicylic acid, J. Mol. Struct. 1116 (2016) 264-271.

[12] L.K. Filak, S. Goschl, P. Heffeter, K.G. Samper, A.E. Egger, M.A. Jakupec, B.K. Keppler, W. Berger, V.B. Arion, Metal-arene complexes with indolo [3,2-c]-quinolines: effects of ruthenium vs osmium and modifications of the lactam unit on intermolecular interactions, anticancer activity, cell cycle, and cellular accumulation, Organometallics 32 (2013) 903-914.

[13] J.C. Chen, G.D. Li, F. Peng, X.M. Jie, G.Z. Dongye, Y. Zhong, R.B. Feng, B.J. Li, J.Y. Qu, Y. Ding, L.M. Chen, Investigation of inducing apoptosis in human lung cancer A549 cells and related mechanism of a ruthenium (II) polypyridyl complex, Inorg. Chem. Commun. 69 (2016) 35-39.

[14] M.R. KaluCerovic, S.Gomez-Ruiz, B. Gallego, E. Hey-Hawkins, R. Paschke, G.N. KaluCerovic, Anticancer activity of dinuclear gallium (III) carboxylate complexes, Eur. J. Med. Chem. 45 (2010) 519-525.

[15] K. Kumar, S. Schniper, A. Gonzalez-Sarrías, A.A. Holder, N. Sanders, D.Sullivan, W.L. Jarrett, K. Davis, F. Bai, N.P. Seeram, V. Kumar, Highly potent anti-proliferative effects of a gallium (III) complex with 7-chloroquinoline thiosemicarbazone as a ligand: Synthesis, cytotoxic and antimalarial evaluation, Eur. J. Med. Chem. 86 (2014) 81-86.

[16] A. Salem, E. Noaman, E. Kandil, A. Badawi, N. Mostafa, Crystal structure and chemotherapeutic efficacy of the novel compound, gallium tetrachloride betaine, against breast cancer using nanotechnology, Tumor Biol. 37 (2016) 11025-11038.

[17]I. Romero-Canelon, L. Salassa, P.J. Sadler, The contrasting activity of iodidoversus chlorido Ruthenium and Osmium Arene Azo- and Imino-pyridine anticancer complexes: controlof cell selectivity, cross-resistance, p53 dependence, and apoptosis pathway, J. Med. Chem. 56 (2013)1291-1300.

[18] K.D. Mjos, C. Orvig, Metallodrugs in medicinal inorganic chemistry, J. Am. Chem. Soc. 114 (2014) 4540-4563.

[19] S.H.V.Rijt, P.J. Sadler, Current applications and future potential for bioinorganic chemistry in the development of anticancer drugs, Drug Discov. Today 14 (2009) 23-24.

[20] L.Banci, I. Bertini, F. Cantini, S. Ciofi-Baffoni, Cellular copper distribution: a mechanistic systems biology approach, Cell Mol. Life Sci. 67 (2010) 2563-2589.

[21]M. Delgado, J. Perez-Miguelsanz, F. Garrido, G. Rodeiguez-Tarduchy, D. Perez-Sala, M.A. Pajares, Early effects of copper accumulation on methionine metabolism, Cell Mol. Life Sci. 65 (2008) 2008-2090.

[22] I.S. MacPherson, M.E.P. Murphy, Type-2 copper-containing enzymes, Cell Mol. Life Sci. 64 (2007) 2887-2899.

[23]S. Kathiresan, S. Mugesh, J. Annaraj, M. Murugan, Mixed-ligand copper (II) Schiff base complexes: the vital role of co-ligands in DNA/protein interactions and cytotoxicity, New J. Chem. 41 (2016) 1267-1283.

[24] F.N. Akladios, S.D. Andrew, C.J. Parkinson, Cytotoxic activity of expanded coordination bis-thiosemicarbazones and copper complexes thereof, J. Biol. Inorg. Chem. 21 (2016) 931-944.

[25] K.E. Prosser, S.W. Chang, F. Saraci, P.H. Le, C.J.Walsby,Anticancer copper pyridine benzimidazole complexes: ROS generation, biomolecule interactions, and cytotoxicity, J. Inorg. Biochem. 167 (2017) 89-99.

[26] W. Villarreal, L. Colina-Vegas, C. Visbal, O. Corona, R.S. Corrêa, J. Ellena, M.R. Cominetti, A.A. Batista, M.Navarro, Copper (I)–Phosphine Polypyridyl Complexes: Synthesis, Characterization, DNA/HSA Binding Study, and Antiproliferative Activity, Inorg. Chem. 56 (2017) 3781-3793.

[27] S. Mignani, N. El Brahmi, L. Eloy, J. Poupon, V. Nicolas, A. Steinmetz, S. EL Kazzouli, M.M. Bousmina, M. Blanchard-Desce, A.M. Caminade, J.P. Majoral,T. Cresteil, Anticancer copper(II) phosphorus dendrimers are potent proapoptoticBax activators, Eur. J. Inorg. Chem. 132 (2017) 142-156.

[28] S.M. Leite, L.M. Lima, S. Gama, F. Mendes, M. Orio, I. Bento, A. Paulo, R. Delgado, O. Iranzo, Copper (II) complexes of phenanthroline and histidine containing ligands: synthesis, characterization and evaluation of their DNA cleavage and cytotoxic activity. Inorg. chem. 55 (2016) 11801-11814.

[29] F.A. Beckford, J. Thessing, A. Stott, A.A. Holder, O.C. Poluektov, L. Li, N.P. Seeram, Anticancer activity and biophysical reactivity of copper complexesof2-(benzo[d][1,3]dioxol-5-ylmethylene)-N-alkylhydrazinecarbothioamides, Inorg. Chem. Commun. 15 (2012) 225-229.

[30] B. Deka, T. Sarkar, S. Banerjee, A. Kumar, S. Mukherjee, S. Deka, K.K. Sailkia, A. Hussain, Novel mitochondria targeted copper (II) complexes of ferrocenylterpyridine and anticancer active 8-hydroxyquinolines

showing remarkable cytotoxicity, DNA and protein binding affinity, Dalton Trans. 46 (2017) 396-409.

[31] J. Dam, Z. Ismail, T. Kurebwa, N. Ganger, L. Harmse, H.M. Marques, A. Lemmerer, M.L. Bode, C.B. de Koning, Synthesis of copper and zinc 2-(pyridin-2-yl)imidazo[1,2-a]pyridine complexes and their potential anticancer activity, Eur. J. Med. Chem. 126 (2017) 353-368.

[32] S. Parveen, S. Tabassum, F. Arjmand, Synthesis of chiral R/S-pseudopeptide-based Cu (II) & Zn (II) complexes for use in targeted delivery for antitumor therapy: enantiomeric discrimination with CT-DNA and pBR322 DNA hydrolytic cleavage mechanism, RSC. Adv. 7 (2017) 6587-6597.

[33] D. Montagner, B. Fresch, K. Browne, V. Gandian, A. Erxleben, A Cu(II) complex targeting the translocator protein: in vitro and in vivo antitumor potential and mechanistic insights, Chem. Commun. 53 (2017) 134-137.

[34] C. Acilan, B. Cevatemre, Z. Adiguzel, D. Karakas, E. Ulukaya, N. Riberio, I. Correia, J.C. Pessoa, Synthesis, biological characterization and evaluation of molecular mechanisms of novel copper complexes as anticancer agents, Biochim.Biophys.Acta 1861 (2017) 218-234.

[35] N.R. Angel, R.M. Khatib, J. Jenkins, M. Smith, J.M. Rubalcava, B.K. Le Daniel Lussier, Z. Chen, F.S. Tham, E.H. Wilson, J.F. Eichler,Copper (II) complexes possessing alkyl-substituted polypyridyl ligands: Structural characterization and in vitro antitumor activity, J. Inorg. Biochem. 166 (2017) 12-25.

[36] J. Lopes, D. Alves, T.S. Morais, P.J. Costa, M.F. Piedade, F. Marques, M.J.Villa de Brito, M. HelanaGarcia, New copper (I) and heteronuclear copper (I)-ruthenium (II) complexes: Synthesis, structural characterization and cytotoxicity, J. Inorg. Biochem. 169 (2017) 68-78.

[37] U.K. Komarnicka, R. Starosta, A. Kyzioł, M. Płotek, M. Puchalska, M. Jeżowska-Bojczuk, New copper (I) complexes bearing lomefloxacin motif: Spectroscopic properties, in vitro cytotoxicity and interactions with DNA and human serum albumin, J. Inorg. Biochem. 165 (2016) 25-35.

[38] M. Jopp, J. Becker, S. Becker, A. Miska, V. Gandin, C. Marzano, S. Schindler, Anticancer activity of a series of copper (II) complexes with tripodal ligands, Eur. J. Med. Chem. 132 (2017) 274-281.

[39] K.C. Park, L. Fouani, P.J. Jansson, D. Wooi, S. Sahni, D.J. Lane, D. Palanimuthu, H.C. Lok, Z. Kovačević, M.L. Huang, D.S. Kalinowski, D.R. Richardson, Copper and conquer: copper complexes of di-2-pyridylketone thiosemicarbazones as novel anti-cancer therapeutics, Metallomics 8 (2016) 874-86.

[40]W.L. Xie, S.M. Xie, Y. Zhou, X.F. Tang, J. Liu, W.Q. Yang, M.H. Qiu. Design and synthesis of novel 5,6-disubstituted pyridine-2,3- dione-3-thiosemicarbazone derivatives as potential anticancer agents, Eur. J. Med. Chem. 81 (2014) 22-27.

[41] J. Qi, Y. Zhang, Y. Gou, Z. Zhang, Z. Zhou, X. Wu, F. Yang, H. Liang, Developing an Anticancer Copper(II) Pro-Drug Based on the His242 Residue of the Human Serum Albumin Carrier IIA Subdomain, Mol.

Pharm. 13 (2016) 1501-1507.

[42] J. Qi, Y. Zhang, Y. Gou, P. Lee, J. Wang, S. Chen, Z. Zhou, X. Wu, F. Yang, H. Liang, Multidrug Delivery Systems Based on Human Serum Albumin for Combination Therapy with Three Anticancer Agents, Mol. Pharm. 13 (2016) 3098-3105.

[43] D.B. Lovejoy, P.J. Jansson, U.T. Brunk, J. Wong, P. Ponka, D. R. Richardson, Antitumor activity of metal-chelating compound Dp44mT is mediated by formation of a redox-active copper complex that accumulates in lysosomes, Cancer Res. 71 (2011) 5871-5880.

[44] A.C.R. Gonçalves, Z.A. Carneiro, C.G. Oliveira, A. Danuello, W. Guerra, R.J. Oliveira, F.B. Ferreira, L.L.W. Veloso-Silva, F.A.H. Batista, J.C. Borges, S. de Albuquerque, V.M. Deflon, P.I.S. Maia, Pt^{II}, Pd^{II} and Au^{III} complexes with a thiosemicarbazone derived from diacethylmonooxime: Structural analysis, trypanocidal activity, cytotoxicity and first insight into the antiparasitic mechanism of action, Eur. J. Med. Chem. 141 (2017) 615-631.

[45] Y. Gou, Z. Zhang, D. Li, L. Zhao, M. Cai, Z. Sun, Y. Li, Y. Zhang, H. Khan, H. Sun, T. Wang, H. Liang, F. Yang, HSA-based multi-target combination therapy: regulating drugs' release from HSA and overcoming single drug resistance in a breast cancer model, Drug Deliv. 25 (2018) 321-329.

[46] B. M. Paterson., P. S. Donnelly, Copper complexes of bis(thiosemicarbazones): from chemotherapeutics to diagnostic and

therapeutic radiopharmaceuticals, Chem. Soc. Rev. 40 (2011) 3005-3018.

[47] F. Yang, H. Liang, Designing anticancer multitarget metal thiosemicarbazone prodrug based on the nature of binding sites of human serum albumin carrier, Future Med. Chem. 10 (2018) 1881-1883.

[48] D. Delphine, M. Shashank, L.F. Sharon, A.C. Michael, Targeting copper in cancer therapy: 'Copper that cancer', Metallomics. 7(2015) 1459-1476.

[49]Q.P. Qin, Z.F. Chen, J.L. Qin, X.J. He, Y.L. Li, Y.C. Liu, K.B. Huang, H. Liang, Studies on antitumor mechanism of two planar platinum(II) complexes with 8-hydroxyquinoline: Synthesis, characterization, cytotoxicity, cell cycle and apoptosis, Eur. J. Med. Chem. 92(2015) 302-313.

[50] X. Ma, J. Han, Q. Wu, H. Liu, S. Shi, C. Wang, Y. Wang, J. Xiao, J. Zhao, J. Jiang, C. Wan, Involvement of dysregulated Wip1 in manganese-induced p53 signaling and neuronal apoptosis, Toxicol. Lett. 235 (2015) 17-27.

[51] J. Ge, C. Wang, X. Nie, J. Yang, H. Lu, X. Song, K. Su, T. Li, J. Han, Y. Zhang, J. Mao, Y. Gu, J. Zhao, S. Jiang, Q. Wu, ROS-mediated apoptosis of HAPI microglia through p53 signaling following PFOS exposure, Environ. Toxicol. Pharmacol. 46 (2016) 9-16.

[52] S. Ikawa, A. Nakagawara, Y. Ikawa, p53 family genes: structural comparison, expression and mutation, Cell Death Differ. 6 (1999) 1154-1161.

[53]Y. Hirohito, J.D. Chen, B. Kapil, H.G. Wang, Regulation of Bax activation and apoptotic response to microtubule-damaging agents by p53 transcription-dependent and -independent pathways, J. Bio. Chem. 279 (2004) 39431-39437.

[54] C.H. Wan, X. Ma, S.S. Shi, J.Y. Zhao, X.K. Nie, J.L. Han, J. Xiao, X.K. Wang, S.Y. Jiang, J.K. Jiang, Pivotal roles of p53 transcription-dependent and -independent pathways in manganese-induced mitochondrial dysfunction and neuronal apoptosis, Toxicol. Appl. Pharmacol. 281 (2014) 294-302.

[55] P. Jiang, W.J. Du, M. Wu, p53 and Bad: remote strangers become close friends, Cell Res. 17 (2008) 283-285.

[56] J.S. Ho, W. Ma, D.Y. Mao, S. Benchimol, p53-dependent transcriptional repression of c-myc is required for G1cell cycle arrest, Mol. Cell. Biol. 25 (2005) 7423-7431.

[57] S.K. Seo, H.O. Jin, S.H. Woo, Y.S. Kim, S. An, J.H. Lee, S.I. Hong, K.H. Lee, T.B. Choe, I.C. Park, Histone deacetylase in hibitors sensitize human non-small cell lung cancer cells to lionizing radiation through acetyl p53-mediated c-myc down-regulation, J. Thorac. Oncol. 6 (2011) 1313-1319.

[58] J.W. Park, Y.J. Choi, M.A. Jang, Y.S. Lee, D. Y. Jun, S. Suh, W.K. Baek, M.H. Suh, I.N. Jin, T. K. Kwon, Chemopreventive agent resveratrol, a

natural product derived from grapes, reversibly inhibits progression through S and G2 phases of the cell cycle in U937 cells, Cancer Lett. 163 (2001) 43-49.

[59] L. Busino, M. Donzelli, M. Chiesa, D. Guardavaccaro, D. Ganoth, N.V. Dorrello, A. Hershko, M. Pagano, G.F. Draetta, Degradation of Cdc25A by b-TrCP during S phase and in response to DNA damage, Nature 426 (2003) 87-91.

[60] T. Tauchi, K. Shin-ya, G. Sashida, M. Sumi, S. Okabe, J.H. Ohyashiki, K. Ohyashiki, Telomerase inhibition with a novel G-quadruplex-interactive agent, telomestatin: in vitro and in vivo studies in acute leukemia, Oncogene 25 (2006) 5719-5725.

[61] J.L. Zhou, Y.J. Lu, T.M. Ou, J.M. Zhou, Z.S. Huang, X.F. Zhu, C.J. Du, X.Z. Bu, L. Ma, L.Q. Gu, Y.M. Li, A.S.C. Chan, Synthesis and evaluation of quindoline derivatives as G-quadruplex inducing and stabilizing ligands inhibitors of telomerase, J. Med. Chem. 48 (2005) 7315-7321.

[62] M. Takakura, S. Kyo, T. Kanaya, H. Hirano, J. Takeda, M. Yutsudo, M. Inoue, Cloning of human telomerase catalytic subunit (hTERT) gene promoter and identification of proximal core promoter sequences essential for transcriptional activation in immortalized and cancer cells, Cancer Res. 59 (1999) 551-557.

[63] S. Kyo, M. Takakura, M. Tanaka, T. Kanaya, M. Inoue,Telomerase activity in cervical cancer is quantitatively distinct from that in its precursor lesions, Int. J. Cancer 79 (1998) 66-70.

[64] K.J. Wu, C. Grandori, M. Amacker, N. Simon-Vermot, A. Polack, J. Lingner, R. Dalla-Favera, Direct activation of TERT transcription by c-MYC, Nat. Genet. 21 (1999) 220-224.

[65] Y. Sagawa, H. Nishi, K. Isaka, A. Fujito, M. Takayama, The correlation of TERT expression with c-myc expression in cervical cancer, Cancer Lett. 168 (2001) 45-50.

[66] W.L. Wong, H. Puthalakath，Bcl-2 Family Proteins: The sentinels of the mitochondrial apoptosis pathway，IUBMB Life 60 (2008) 390-397.

[67] M. Kaghad, H. Bonnet, A. Yang, L. Creancier, J.C. Biscan, A. Valent, A. Minty, P. Chalon, J.M. Lelias, X. Dumont, P. Ferrara, F. McKeon, D. Caput, Monoallelically expressed gene related to p53 at 1p36, a region frequently deleted in neuroblastoma and other human cancers, Cell 90 (1997) 809-819.

[68] E.H. Cheng, M.C. Wei, S. Weiler, R.A. Flavell, T.W. Mak, T. Lindsten, S.J. Korsmeyer, BCL-2, BCL-X(L) sequester BH3 domain-only molecules preventing BAX- and BAK-mediated mitochondrial apoptosis, Mol. Cell 8 (2001) 705-711.

[69] S.H. Inayat−Hussain, B.O. Annuar, L.B. Din, A.M. Ali, D. Ross, Loss of mitochondrial transmembrane potential and caspase-9 activation during apoptosis induced by the novel styryl-lactone goniothalamin in HL-60 leukemia cells, Toxicol. In Vitro 17 (2003) 433-439.

[70]K. Sinha, J. Das, P.B. Pal, P.C. Sil, Oxidative stress: the mitochondria-dependent and mitochondria-independent pathways of apoptosis, Arch. Toxicol. 87 (2013) 1157-1180.

[71]P. Li, Q.L. Zhao, L.H. Wu, P. Jawaid, Y.F. Jiao, M. Kadowaki, T. Kondo, Isofraxidin, a potent reactive oxygen species (ROS) scavenger, protects human leukemia cells from radiation-induced apoptosis via ROS/mitochondria pathway in p53-independent manner, Apoptosis 19 (2014) 1043-1053.

[72]L. Diebold, N.S. Chandel, Mitochondrial ROS regulation of proliferating cells, Free Radical Bio. Med. 100 (2016) 86-93.

[73] D. Green, G. Kroemer, The central executioners of apoptosis: caspases or mitochondria? Trends Cell Biol. 8 (1998) 267-271.

[74] M. Kurokawa1, S. Kornbluth, Caspases and Kinases in a Death Grip, Cell. 138 (2009) 838-853.

[75] C. Stroh, K. Schulze-Osthoff, Death by a thousand cuts: an ever increasing list of caspase substrates, Cell Death Differ. 5 (1998) 997-1000.

[76] J. Wang, Y. Gou, Z. Zhang, P. Yu, J. Qi, Q. Qin, H. Sun, X. Wu, H. Liang, F. Yang, Developing an Anticancer Copper(II) Multitarget Pro-Drug Based on the His146 Residue in the IB Subdomain of Modified Human Serum Albumin, Mol. Pharm. 15 (2018) 2180-2193.

[77] Q.Y. Mo, J.G. Deng, Y.N. Liu, G.D. Huang, Z.W. Li, P. Yu, Y. Gou, F. Yang, Mixed-ligand Cu(II) hydrazone complexes designed to enhance anticancer activity, Eur. J. Med. Chem. 156 (2018) 368-380.

[78] J.X. Qi, Y. Gou, Y. Zhang, K. Yang, S.F. Chen, L. Liu, X.Y. Wu, T. Wang, W. Zhang, F. Yang, Developing Anticancer Ferric Prodrugs Based on the N-Donor Residues of Human Serum Albumin Carrier IIA Subdomain, J. Med. Chem. 59 (2016) 7497-7511.

[79] O.V. Dolomanov, L.J. Bourhis, R.J. Gildea, J.A.K.Howard, H. Puschmann, OLEX2: a complete structure solution, refinement and analysis program, J. Appl. Crystallogr. 42 (2009) 339-341.

[80]J. Carmichael, W.G. DeGraff, A.F. Gazdar, J.D. Minna, J.B. Mitchell, Evaluation of a tetrazolium-based semiautomated colorimetric assay: assessment of chemosensitivity testing, Cancer Res. 47 (1987) 936-942.

[81]E. Schreiber, P. Matthias, M.M. Mueller, W. Schaffner, Rapid detection of octamer binding proteins with ‘mini-extracts’ prepared from a small number of cells, Nucleic Acids Res. 17 (1989) 6419.

[82]X.X. Bu, F.Q. Jia, W.F. Wang, X.L. Guo, M.C. Wu, L.X. Wei, Coupled down-regulation of mTOR and telomerase activity during fluorouracil-induced apoptosis of hepatocarcinoma cells, BMC Cancer 7 (2007) 208.

Figure legends

Scheme 1 Synthetic routes for C1-C5

Figure 1 The chemical structures of C1-C5.

Figure 2 Metal contents in whole MIG80-3 cells deducting blank control and different fraction was measured by ICP-MS after the MIG80-3 cells were treated with C1-C5 (0.8 μM) for 24 h, The values were relative to C1 (*P < 0.05).

Figure 3(A) Effect of the cell cycle treated with (a) control; (b) C1-6μM; (c) C1-12μM); (d) C4-0.4μM; (e) C4-0.8μM for 48 h. (B) Western blot analysis the levels of Cdc25A, Cyclin A2, CDK2, p27 and p21. (C) Densitometric analysis of the expression of Cdc25A, Cyclin A2, CDK2, p27 and p21.The percentage values were relative to the control (*P < 0.05).

Figure 4 (A) The protein levels of c-myc and hTERT in MGC80-3 cells treated with C1 (6/12 μM) and C4 (0.4/0.8 μM) for 24 h, respectively. (B) Densitometric analysis of c-myc and hTERT (*P < 0.05). (C)The influence on the telomerase activity in the MGC80-3 cells treated with C1 (12 μM) and C4 (0.8 μM).

Figure 5 (A) Western blot analysis the levels of Apaf-1, Bcl-2, Bax, Bad, p53 and Cyt C after treated with (6/12 μM) and C4 (0.4/0.8 μM) for 24 h. (B) Densitometric analysis of the expression of Apaf-1, Bcl-2, Bax, Bad, p53 and Cyt C. The percentage values are those relative to the control (*P < 0.05). (C) Apoptosis of MIG80-3 cells treated with C1 and C4. (a) Control; (b) C1=6 μM; (c) C1=12 μM; (d) C4=0.4 μM; (e) C4=0.8 μM.

Table 1

Table1 Crystal Data of the five Pt(II) complexes.

Identification code	C1	C2	C3	C4	C5
Empirical formula	$C_8H_9ClCuN_4S$	$C_{13}H_{11}CuN_5O_3S$	$C_{12}H_{15}BrCuN_4S$	$C_{10}H_{15}BrCuN_4OS$	$C_{12}H_{17}ClCuN_4OS$
Formula weight	292.24	380.87	390.79	382.77	364.35
Temperature/K	296.15	296.15	296.15	296.15	296.15
Crystal system	triclinic	monoclinic	monoclinic	triclinic	triclinic
Space group	*P*-1	*C*2/*c*	$P2_1/c$	*P*-1	*P*-1
a (Å)	6.7305(9)	17.627(2)	10.992(7)	7.6723(4)	7.464(3)
b (Å)	9.306(12)	16.055(2)	14.559(10)	9.6352(5)	9.748(4)
c (Å)	9.439(10)	13.663(18)	9.122(6)	9.7622(5)	10.352(5)
α (°)	106.595(10)	90	90	101.585(5)	93.078(6)
β (°)	106.835(10)	129.523(2)	95.173(10)	96.629(5)	95.765(6)
γ (°)	95.062(11)	90	90	95.743(5)	98.652(6)
V (Å^3)	532.78(12)	2982.5(7)	1453.8(17)	696.58(7)	739.0(6)
Z	2	8	4	2	2
ρ_{cal}/cm^3	1.822	1.696	1.785	1.825	1.637
μ(Mo-Kα) (mm^{-1})	2.465	1.627	4.385	4.579	1.799
F(000)	294	1544	780	382	374
Data/restraints/parameters	1869/0/137	3059/0/208	2951/0/179	2450/0/170	3031/0/186
Goodness-of-fit on F^2	1.105	0.873	0.84	1.069	1.134
Final *R* indexes [$I>=2\sigma(I)$]	R_1=0.0349	R_1=0.0399	R_1=0.0272	R_1=0.0264	R_1=0.0282
	*wR*2=0.0936	*wR*2=0.1114	*wR*2=0.0946	*wR*2=0.0670	*wR*2=0.0892
CCDC NO.	1015147	1829668	1829670	1829669	1829671

Table 2

Table 2 IC_{50} (μM) values of Cu(II) complexes toward the cell lines.

Cells	MGC80-3	NCI-H460	Hep-G2	SK-OV-3	HL-7702
Ligand1	19.04±0.43	16.83±0.79	12.52±1.51	13.33±0.97	19.85±0.41
Ligand2	7.83±0.65	6.71±0.83	6.98±0.36	7.03±0.28	8.41±0.27
Ligand3	4.12±0.25	4.31±0.47	4.95±0.40	4.39±0.23	6.21±0.26
Ligand4	3.57±0.17	3.98±0.51	3.49±0.33	3.75±0.19	4.28±0.37
Ligand5	4.32±0.31	4.49±0.72	5.58±0.57	4.51±0.41	7.15±0.46
C1	12.11±0.82	11.57±1.25	6.81±1.35	7.93±0.73	13.37±1.85
C2	1.30±0.47	1.52±0.48	1.78±0.43	1.92±0.45	2.39±0.27
C3	1.09±0.42	1.39±0.37	1.60±0.46	1.26±0.47	1.76±0.35
C4	0.84±0.49	1.28±0.46	1.31±0.24	1.18±0.44	1.68±0.45
C5	1.11±0.33	1.43±0.34	1.69±0.47	1.29±0.48	2.08±0.44
Cis-platin	16.84±0.45	18.11±0.38	17.23±0.24	16.72±1.25	10.79±0.51

Scheme

Click here to download high resolution image

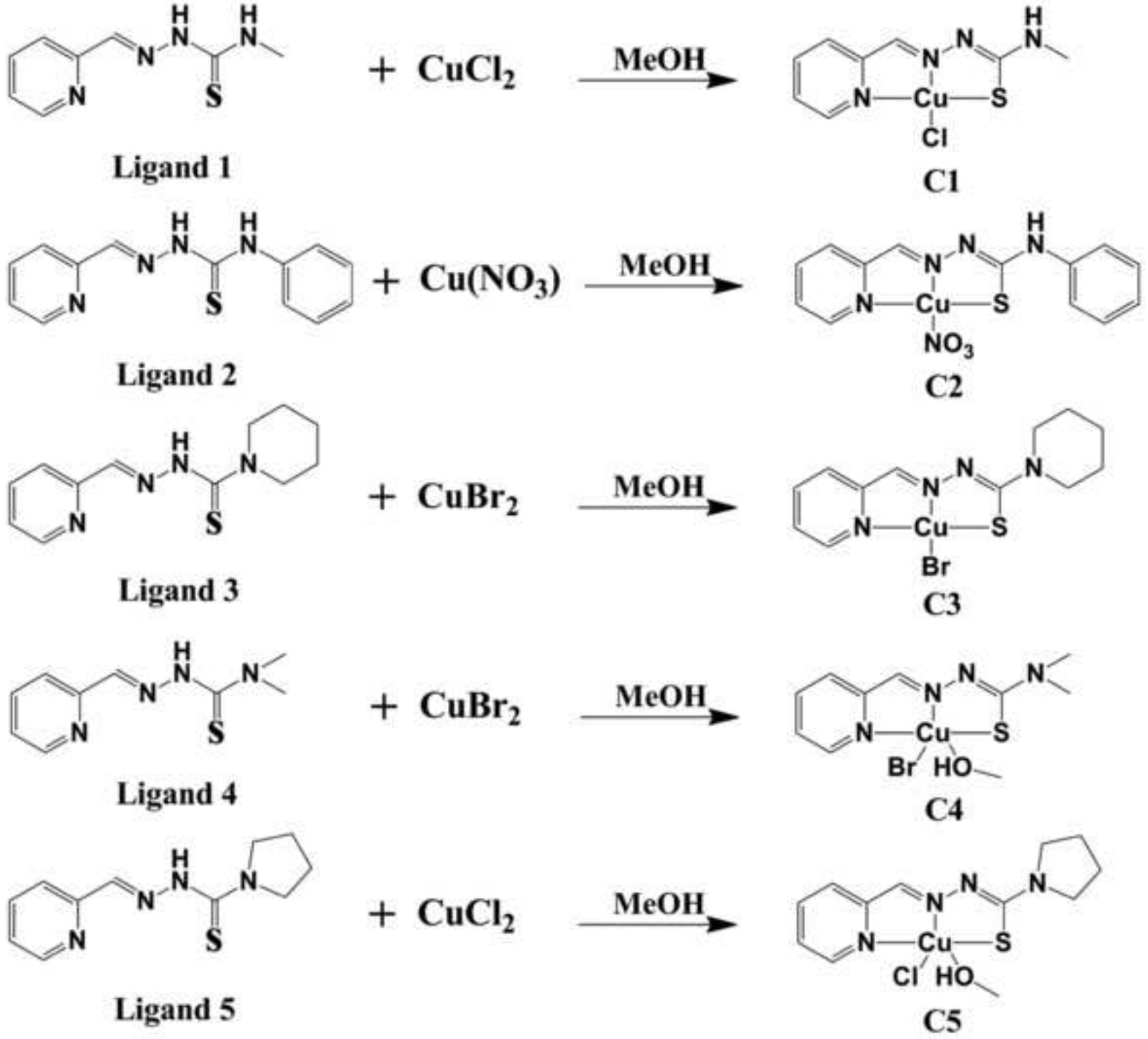

Figure 1

Click here to download high resolution image

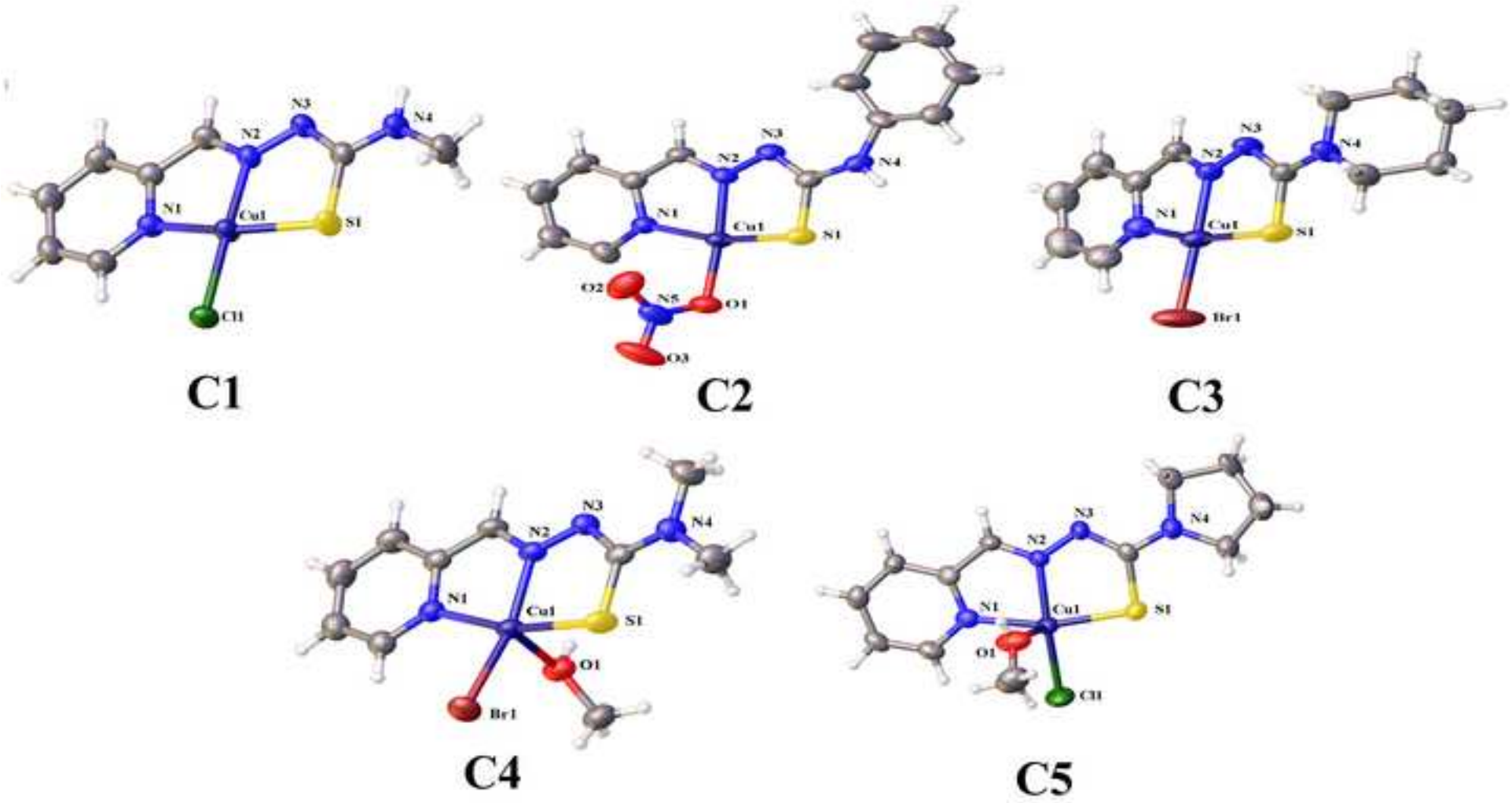

Figure 2

Click here to download high resolution image

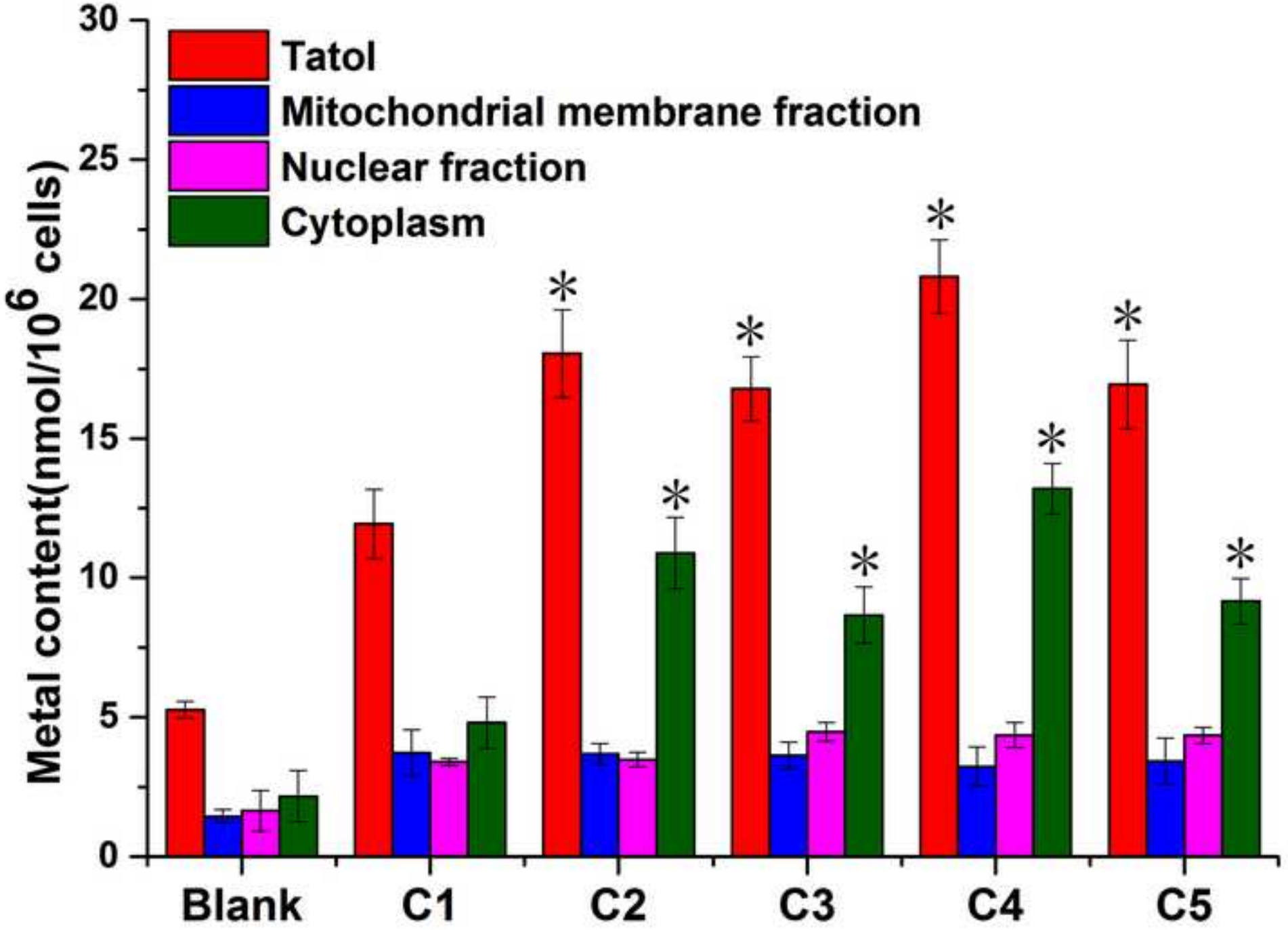

Figure 3

Click here to download high resolution image

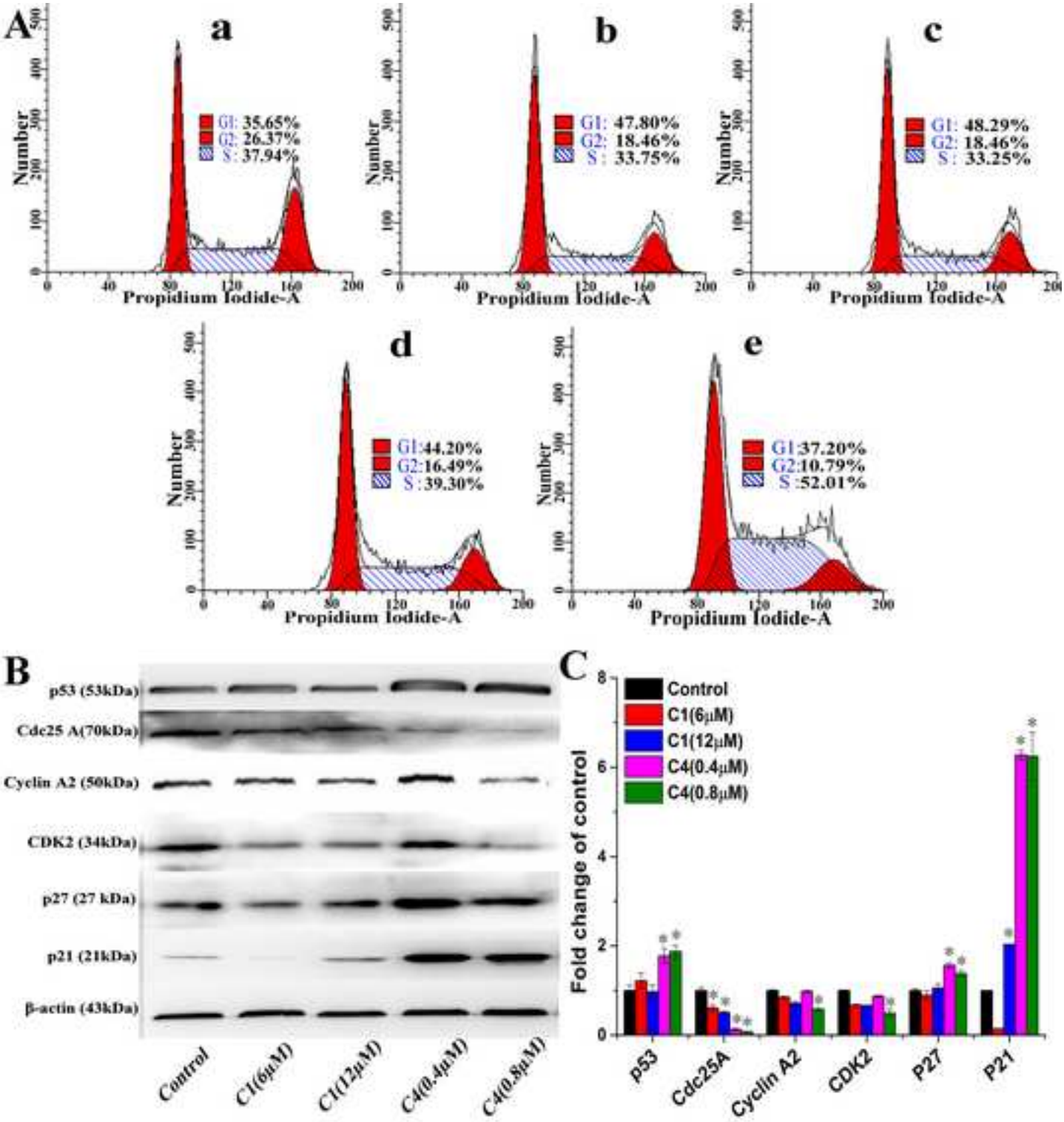

Figure 4

Click here to download high resolution image

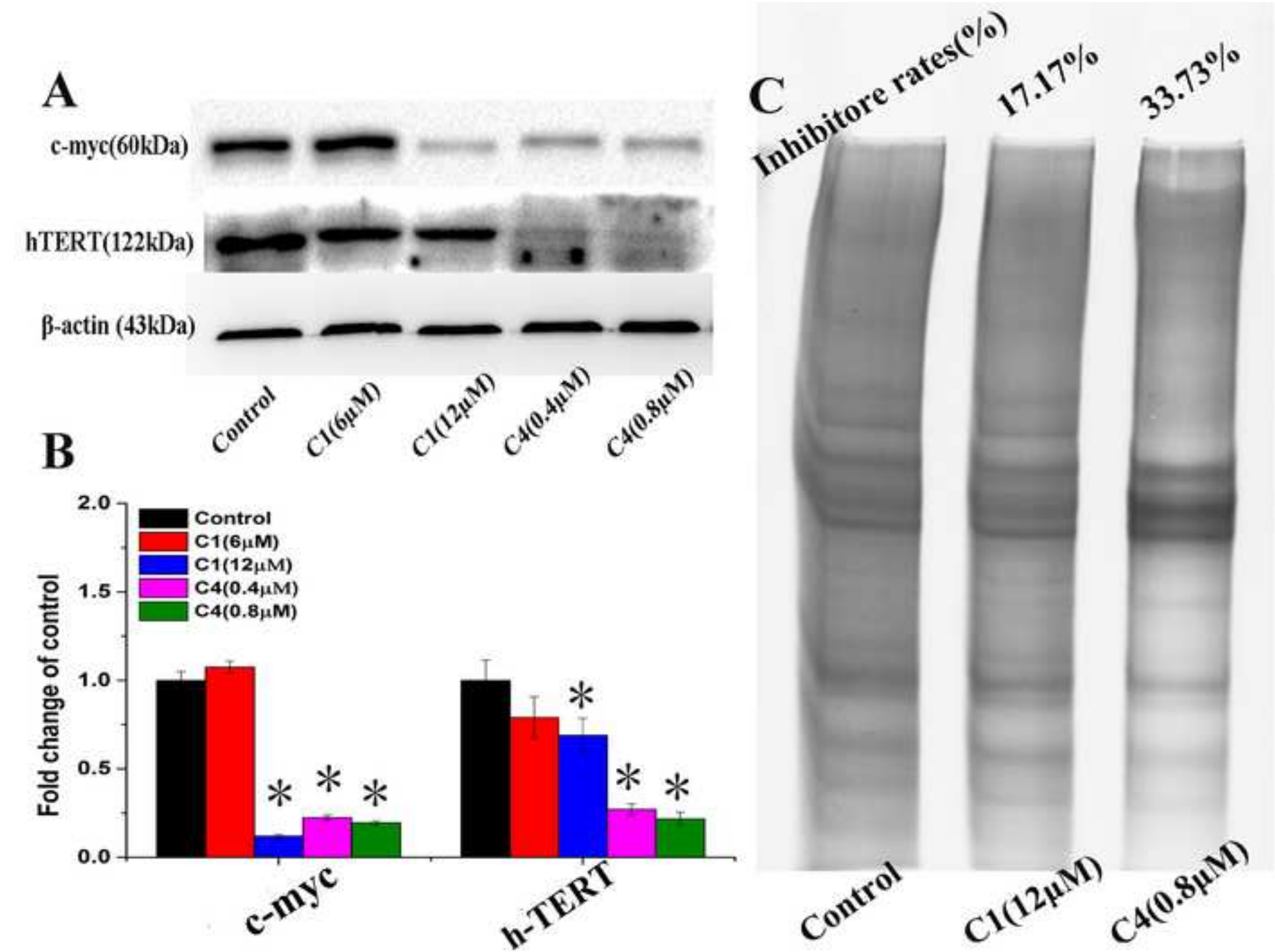

Figure 5

Click here to download high resolution image

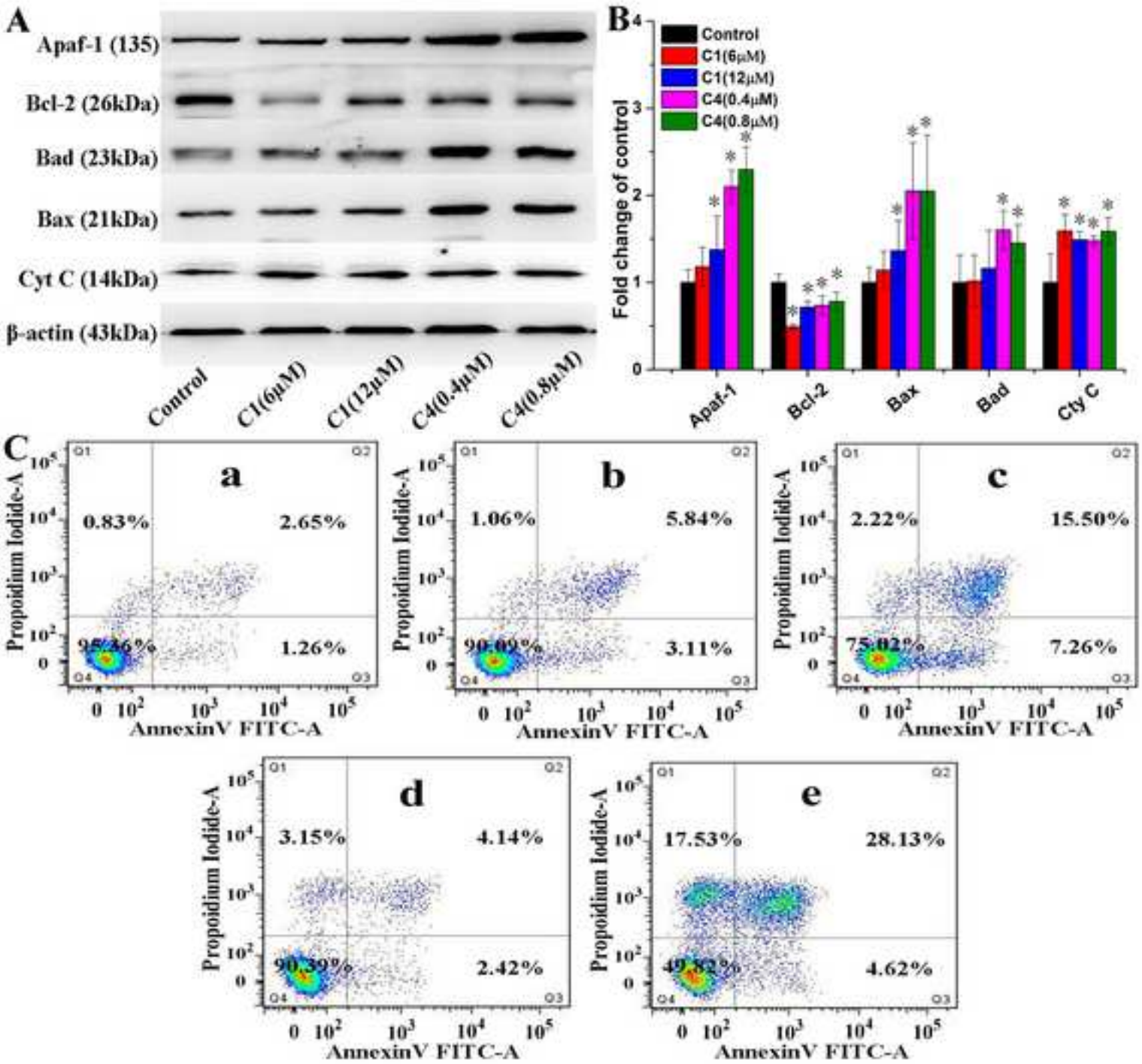

Supplementary Material - For Publication Online

Click here to download Supplementary Material - For Publication Online: Supporting Information.docx